The Formation of Comma Vortices in a Tropical Numerical Simulation Model

ROBERT E. TULEYA AND YOSHIO KURIHARA

Geophysical Fluid Dynamics Laboratory/NOAA, Princeton University, Princeton, NJ 08542

(Manuscript received 6 September 1983, in final form 9 December 1983)

ABSTRACT

A detailed analysis of a numerically simulated tropical disturbance displays a comma-shaped pattern at the mature stage in the low-level vorticity, surface convergence, mid-level upward motion and precipitation fields. This study reveals that the high wind side of the disturbance is the favorable region for the formation of the tail of the comma pattern. The β effect retards the development of the comma shape in the case of easterly environmental winds and enhances it in the case of westerlies. Analysis of the vorticity field suggests that the initial shape and intensity of the perturbation can influence the wind pattern of an evolving disturbance. Although some indications of band-like features exist in the wind field for dry experiments with no lower-boundary fluxes, surface fluxes of heat, moisture and momentum are found to be vital ingredients for the formative process of the distinct comma shape of the disturbance.

1. Introduction

a. Phenomenology of comma-shaped atmospheric vortices

The age of satellites and radar have enabled meteorologists to examine the detailed structure of atmospheric disturbances. Particular atmospheric phenomena have unique signatures which can be particularly useful in practical forecasting and in diagnostic analysis over data sparse regions (e.g., Dvorak, 1975). One common feature appearing over both extratropical and tropical oceans is a comma-shaped atmospheric disturbance with horizontal scale 500–1000 km. This phenomenon is often referred to simply as a "comma disturbance" or a "comma vortex."

Reed (1979) has presented a thorough summary of the state-of-the-art understanding of comma disturbances over extratropical oceans and various possible sources of energy of those disturbances. Locatelli *et al.* (1982) have investigated this phenomenon in more detail. In general these extratropical phenomena are associated with a surface pressure trough. The band or comma tail emanates from the vortex center. It represents an area of various degrees of convection. Banded structure is typical of tropical systems as well, and often a distinct comma shape similar to the aforementioned extratropical systems can be observed (e.g., Dvorak, 1975; Brandli, 1976; Anderson, 1974; Lawrence and Pelissier, 1982). A kinematic explanation for the formation of the comma shape suggested by R. Weldon of the National Earth Satellite Service as described by Reed (1979) is based on the idea of radially nonuniform advection of cloud patterns. The evolution of a comma vortex and its dependence on environmental flow has not been investigated extensively.

b. Capability of numerical models to simulate comma vortices

Early model simulations have shown a potential impact of both the latitudinal variation of Coriolis parameter (the β effect) and the environmental flow on the structure of tropical disturbances. Anthes and Hoke (1975) stated that the nearly stationary band found in their hurricane model may be related to the confluence zone which developed in the initially circular vortex in their barotropic experiments. Apparently, the β effect produced a preferred location where the confluence pattern can be induced. On the other hand, in a nested-grid experiment on an f-plane (f = constant; f is the Coriolis parameter), some slow-moving bands associated with confluence and rainfall were obtained by Jones (1977). He hypothesized that these bands are a result of the interaction between a vortex and its environmental steering current. The work of Tuleya and Kurihara (1981, hereafter TK) revealed a dependence of the structure of developing tropical depressions on flow direction. For easterly winds an amorphous depression evolved with little evidence of a comma-type structure. However, for westerly winds a more vigorous disturbance developed with a distinct comma shape. Fig. 1 displays the results of TK for easterly, zero, and westerly uniform flow for the low level (σ = 0.95, ~435 m; σ is the pressure normalized by the surface pressure) vorticity field. From TK, it can be speculated that the β effect, interacting with the environmental flow, can cause sig-

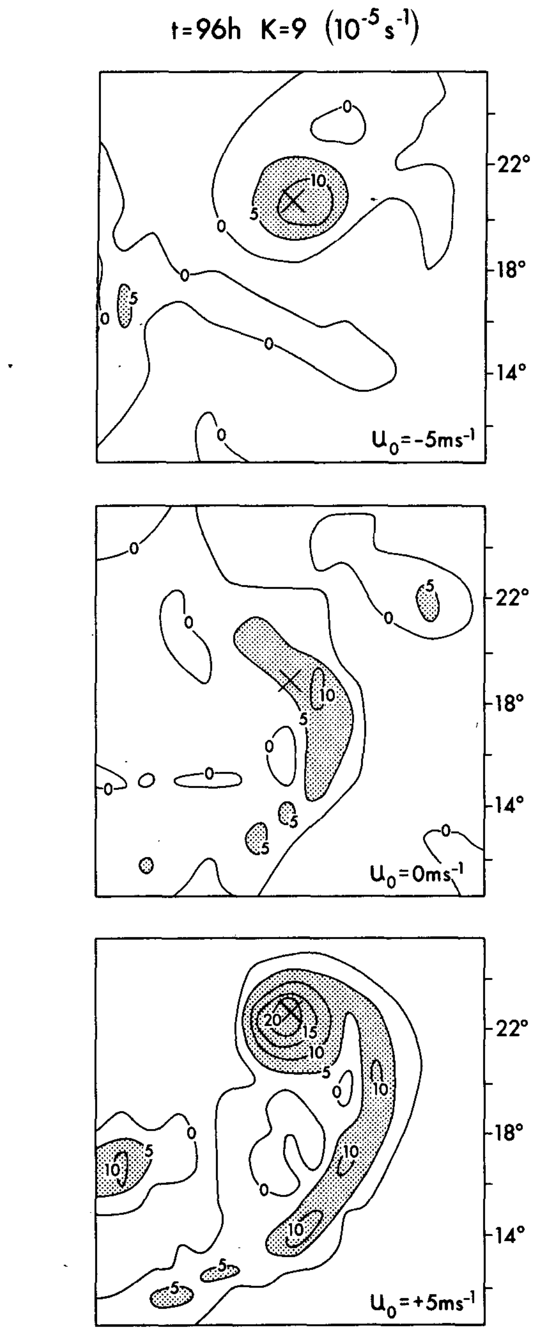

FIG. 1. Distribution of level 9 (σ = 0.95) vorticity (10^{-5} s^{-1}) at 96 h for experiments with u_0 = −5, 0, and +5 m s^{-1} (top to bottom), respectively. A positive u_0 denotes westerlies.

nificant changes in the shape and characteristics of tropical disturbances, at least for the initial conditions which were specified in their experiments.

c. Relation between observed comma disturbances and their propagation direction

One can correlate the observed shape of tropical disturbances with their propagation direction. This was done for the Atlantic and Caribbean regions for the years 1979–81. Disturbances were included and classified as eastward propagating, westward propagating, and northward propagating if their propagation track was within 30° of the direction specified. The disturbance tracks used were those taken from the annual Atlantic hurricane summaries by Hebert (1980) and Lawrence and Pelissier (1981 and 1982). The structure types, comma open to the west, east, south and others were subjectively determined from TIROS-N and NOAA 6 and 7 infrared and visible images. One sees from this summary in Fig. 2 that 22 of 39 cases fall into the amorphous shape category and that almost half the cases (17) are of the westward propagation category. This is not unexpected because of the complex structure of tropical systems and the predominance of tropical easterlies in this region. Nevertheless, there does seem to be a tendency for the open-to-the-west comma structure to occur with disturbances moving eastward. If one assumes that the propagation direction of these observed tropical systems was largely determined by the mean steering flow, the preceding results are consistent with the results of TK. In addition, there is a tendency for open-to-the-south and open-

	Westward Propagating	Eastward Propagating	Northward Propagating
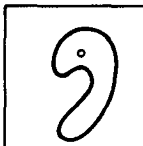	0	4	1
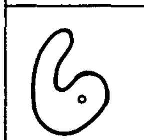	3	0	1
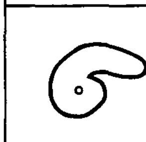	2	1	5
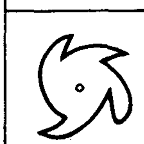	12	7	3

FIG. 2. Number of storms with specified shapes versus their direction of propagation. Data are for tropical systems for the years 1979–81 for the tropical and subtropical Atlantic region. Propagation directions indicated are within ±30° of the angles as taken from the yearly summaries of Atlantic hurricanes by Hebert (1980) and Lawrence and Pelissier (1981, 1982). Shapes are subjectively determined from IR and visible NOAA 6, 7 and TIROS-N satellite images. Bottom row refers to amorphous or many-banded type tropical systems.

to-the-east comma structures to be associated with northward and westward propagation, respectively.

d. Objective of this study and the models used

In this study, the results of TK will be analyzed in Section 2 in order to examine the band structure and formation sequence of the comma vortex in detail. In Section 3 the individual and combined roles of the mean flow direction, the β effect, and the diabatic processes and associated surface fluxes in the formation of the comma vortices will be investigated with the use of two types of numerical models; i.e., a spherical model and an f-plane model. The spherical model consists of a latitude–longitude grid with variable f in contrast to the f-plane model consisting of a rectangular grid with constant f.

The model used in TK is a spherical model with a 25° × 25° channel domain centered at 18°N. The model resolution is 0.625° in the horizontal and has 11 levels in the vertical. It is initialized with a prescribed low level wave-type perturbation superposed on a basic zonal current defined by (3.1) of TK. The numerical results presented in Section 2 are those obtained from the initial condition in which the horizontally nonuniform part of the environmental flow, u_1 in (3.1) of TK, is neglected and the uniform part $u_0(\sigma)$ assumed constant. The spherical model used in Section 3 is identical with that of TK. The uniform basic flow at the initial time is either easterly, westerly or zero (no wind). The additional model used in Section 3 is an f-plane model with $f = 2\Omega \sin 18°$, where Ω is the earth rotation rate, and with a horizontal domain size, 2800 km², being nearly equal to that of the spherical model.

2. Band analysis

a. Horizontal structure

The vorticity field of the disturbance at its mature stage in the experiment of TK with $u_0 = +5$ m s^{-1} (westerlies) is presented in the bottom part of Fig. 1. The low-level wind field for the same disturbance with the areas of instantaneous precipitation > 1.5 mm h^{-1} superposed is shown in Fig. 3. It is clearly seen that a comma pattern with the band width ~ 200 km is observed in the precipitation field as well as the vorticity field and the precipitation band is well correlated with a wind shift and convergence zone. Strong southerly to southwesterly winds prevail at the leading edge of the comma tail precipitation band. Along the back half of this band, a weak pressure trough (~0.5 mb) with locally increasing pressure is found. The center line of the relative vorticity band (Fig. 1) is located

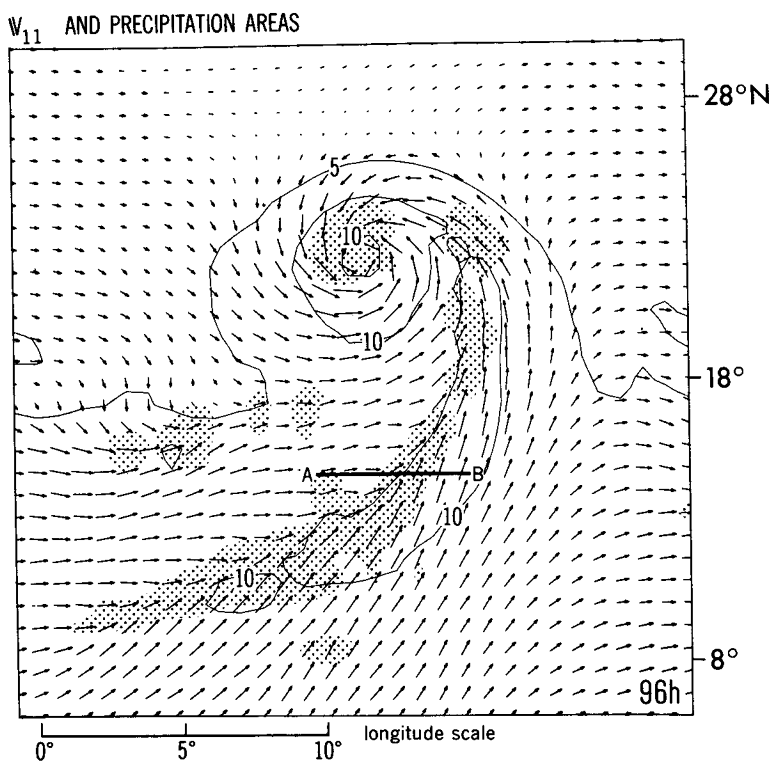

FIG. 3. Isotachs (in m s^{-1}) and wind vectors for low-level (σ = 0.992) wind flow for the experiment with u_0 = +5 m s^{-1}. The time of 96 h corresponds to that of Fig. 1. Shading indicates a precipitation rate greater than 1.5 mm h^{-1}. Line AB is explained in text.

slightly inside the western edge of the precipitation band.

b. Vertical structure

In order to analyze the vertical structure of the comma band, a vertical cross section is taken along the line AB indicated in Fig. 3. This analysis, shown in Fig. 4, displays a deep upward motion coincident with high relative humidity. Additional analysis reveals upper-level (~250 mb) anticyclonic, divergent outflow at and ahead of the comma band. A schematic description of the band is presented in Fig. 5. As opposed to the spiral band analysis of Kurihara and Tuleya (1974), this band is vertically deep with convective processes apparently playing a more dominant role. Unlike the fast-propagating spiral bands described by Kurihara and Tuleya (1974), the band feature is pronounced in the vorticity field as indicated in Fig. 1; the band is associated with a pressure trough; and its speed of movement is comparable with the propagation speed of the main vortex and the environmental flow.

c. Time history of the band formation

The time history of this disturbance and the development of the comma-shaped band is shown in Fig. 6. It is apparent that the vorticity axis (dashed lines) and the developing surface pressure low center (marked by crosses) are not initially aligned. The developing disturbance propagates east–southeast until 36 h and northeastward afterward with the axis of the positive vorticity region elongating and connecting with the surface pressure center by 48 h. Several degrees latitude from the surface center, the band axis assumes a north-east–southwest tilt, whereas close to the center the vorticity axis continues to rotate cyclonically about the surface pressure center.

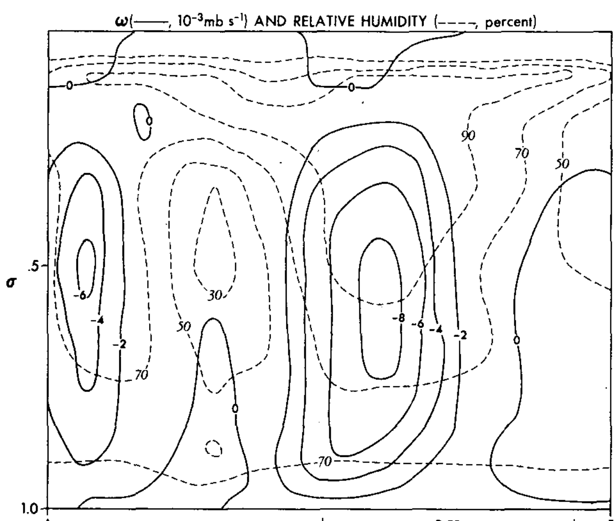

FIG. 4. Vertical cross section of $\omega = dp/dt$, (solid lines) in 10^{-3} mb s^{-1} and relative humidity (dashed lines) in percent along the line AB shown in Fig. 3. Line AB extends through the tail of the comma disturbance.

3. Band formation mechanisms

a. Band formation on an f-plane

One question which immediately comes to mind is the role of the β effect in the formation of the comma disturbance. One cannot use the results of TK to discuss whether or not the β effect was a necessary ingredient in comma formation. In order to answer this question a series of experiments analogous to those of TK were performed on an f-plane, i.e., $\beta = 0$. As previously mentioned, the model used was nearly identical to that of TK except for the f-plane assumptions and the related changes from a spherical geometry to a rectangular domain.

One sees in Fig. 7, the f-plane analogue of Fig. 1, that comma vortices form in both easterly ($u_0 = -5$ m s^{-1}) and westerly ($u_0 = +5$ m s^{-1}) cases. As far as the present experiments are concerned, the band forms on the high wind side of the disturbance. Higher winds produce more evaporation and are probably associated with more convergence in the vicinity of the vorticity axis which leads to band formation. The patterns in Fig. 7 in easterly and westerly cases are almost rotationally symmetric with respect to each other, as they should be. The differences in the evolution of these three patterns in Fig. 7 are due to differences in the air–sea interaction processes and their impact on the vortex-environmental flow interaction. It can be speculated that the patterns obtained and the differences among these patterns depend on the initial and transient strength of the disturbance relative to the mean flow. In this study, the initial perturbation was similar in magnitude to that of the basic flow. For relatively more intense perturbations, the direction of the basic flow may have less impact on the evolution of disturbance shape. If a strong wind shear is present in either the disturbance or the basic flow, it will influence the band structure and may even retard the band formation.

Comparison between Fig. 7 and Fig. 1 shows that the comma pattern on the f-plane is less distinct than that in the case of westerlies on the sphere, and clearly more distinct than the amorphous pattern in the case of easterlies on a sphere. The case of no zonal flow ($u_0 = 0$ m s^{-1}; Fig. 7, center) indicates little formation of a pattern of comma shape related to the initial disturbance center, with the initial low-level disturbance pattern splitting and moving away. This is probably related to boundary-layer processes because aloft the initial pattern remains more intact. There is little similarity between the $u_0 = 0$, $\beta = 0$ and the $u_0 = 0$, $\beta \neq 0$ case shown in Fig. 1 (center). As described by Anthes and Hoke (1975), the β effect can induce a confluence zone on the eastern side of a vortex through

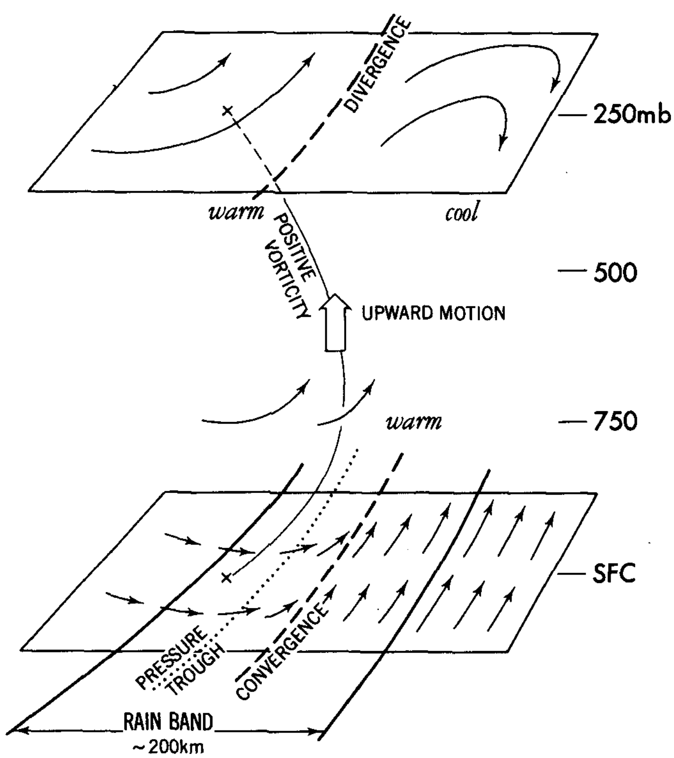

FIG. 5. Schematic figure of the band structure of the comma disturbance simulated for the experiment with $u_0 = +5$ m s^{-1} for the mature stage. Various quantities are shown at 250 mb and at the surface. The position of maximum vorticity at intermediate levels is shown by the solid line connecting the position at different levels. The region of maximum upward motion is indicated by a large arrow at ~600 mb.

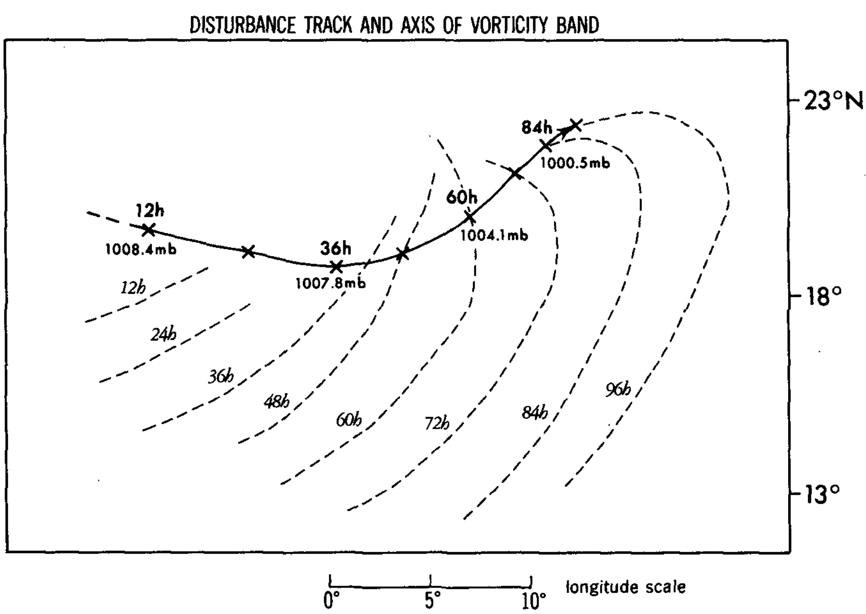

FIG. 6. Storm track (solid line) of the disturbance for the experiment with $u_0 = +5$ m s^{-1}. Positions of surface pressure minimum are marked by crosses every 12 h. The axes of level 9 ($\sigma = 0.992$) maximum vorticity are indicated by dashed lines.

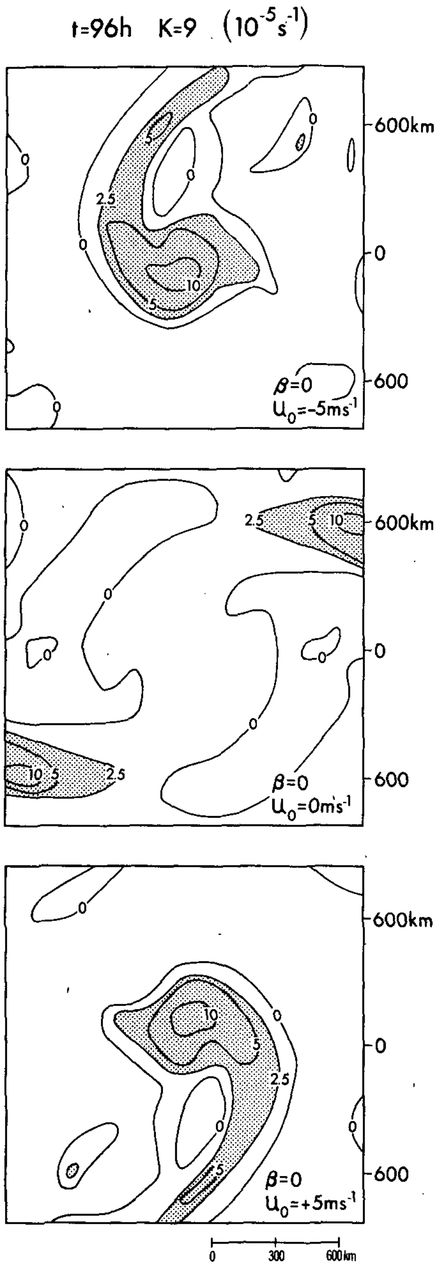

FIG. 7. As in Fig. 1 but for f-plane experiments with $\beta = 0$.

the formation of a negative vorticity area yet farther to the east. Apparently, the confluence pattern contributes to the formation of a surface convergence zone and maintains it close to the vortex. The maximum vorticity area east of the disturbance in Fig. 1 (center) is formed by this mechanism.

In summary, the present experiments, together with those of TK, indicate that 1) a comma pattern can develop on an f-plane with the band or comma tail on the high wind side of the disturbance, i.e., the β effect is not a necessary factor for comma vortex formation for the wave-type initial perturbation prescribed in this study; and 2) the β effect can induce comma formation in case of no mean flow and enhances comma formation in mean westerly flow and suppresses formation in easterly flow. In some additional experiments with circular initial perturbations on a sphere, it was also found (not shown) that a distinct comma pattern evolves in uniform westerlies but not in uniform easterlies.

b. *Vorticity advection and the β effect*

In order to investigate the purely dynamic processes involved in comma shape formation, the rectangular f-plane model of the previous section was integrated with the same initial conditions for the temperature and wind field for a westerly environmental current of $u_0 = +5$ m s^{-1}. In this case, however, diabatic terms such as radiation and condensation were excluded as well as all surface fluxes. The initial vorticity pattern and the low-level wind-speed distribution are shown in the left part of Fig. 8 and the subsequent 48 h fields in the right part. The initial noncircular vorticity pattern rotates counterclockwise approximately 45 degrees around the disturbance center as the wind maximum shifts from south to southeast. This is a case of simple nonlinear vorticity advection. The corresponding wind maximum at 48 h to the southeast of the vorticity center may be considered a precursor of the band of a comma disturbance, although advection of a noncircular pattern is neither necessary nor sufficient for comma formation.

Next, in order to understand how the β term changes this essentially barotropic pattern, two experiments were performed which are identical to the spherical domain ($\beta \neq 0$) experiments of Section 2, except that again neither moisture, diabatic processes, nor surface fluxes were included. Fig. 9 presents the low-level wind analyses for the easterly ($u_0 = -5$ m s^{-1}) and westerly ($u_0 = +5$ m s^{-1}) cases for 0, 24 and 48 h. Although the evolutions of the vorticity patterns of both experiments (figures not shown) are nearly identical to each other and to that shown in Fig. 8, the evolved wind patterns, with either one of them being rotated 180 degrees, are no longer similar to each other. In the case of westerlies ($u_0 = +5$ m s^{-1}), the 7.5 m s^{-1} contour is elongated and extends north beyond the latitude of the disturbance center. At 48 h a line of high wind curvature extends from northeast to southwest, west of this wind maximum. With easterlies ($u_0 = -5$ m s^{-1}), two distinct lines of high curvature exist, one extending northeast to southwest through the disturbance center and a second trough northwest to southeast $\sim 5°$ west of the disturbance. The 7.5 m s^{-1} contour of the $u_0 = -5$ m s^{-1} case encloses an area smaller than that of the $u_0 = +5$ m s^{-1} case with little evidence of extension toward the latitude of the disturbance center.

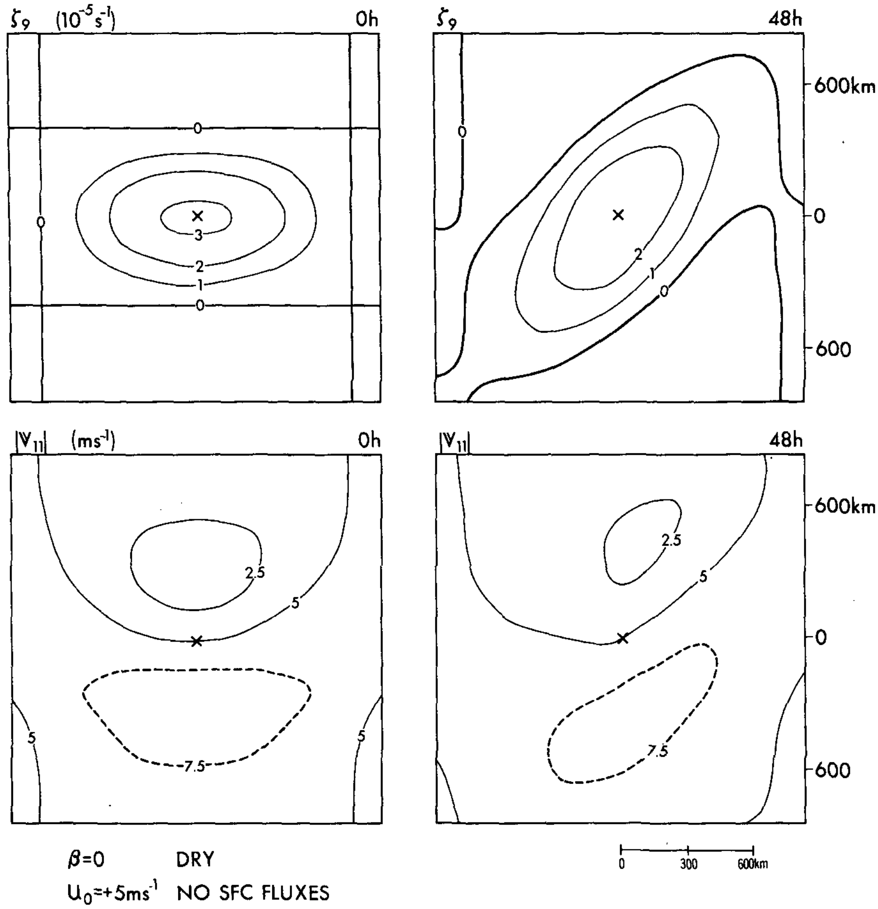

FIG. 8. Distribution of initial (left column) and 48 h (right column) level 9 ($\sigma = 0.95$) vorticity (10^{-5} s^{-1}, top row) and low-level ($\sigma = 0.992$) wind speed (m s^{-1}, bottom row) for the dry f-plane experiment with no surface fluxes and with $u_0 = +5$ m s^{-1}.

In these dry, no surface flux experiments the net vorticity tendency is nearly equal to the term $-(\mathbf{v} - \mathbf{c}) \cdot \nabla(f + \zeta)$, the horizontal advection relative to the disturbance phase velocity $\mathbf{c}$. The wind $\mathbf{v}$ is composed of the meridional and zonal components v and u respectively and ζ is the relative vorticity. The contributions of the other terms in the vorticity budget are negligibly small. In order to investigate the role of the mean flow and disturbance separately, the wind and vorticity are separated into mean and perturbation components, e.g., $\bar{v} = v + v'$ where a bar denotes a longitudinal mean and a prime the deviation from that mean. In the experiments to be discussed here, one can assume that $u = u_0 =$ constant and that $\bar{v} = 0$. Thus the advection term can be written as

$$-(\mathbf{v} - \mathbf{c}) \cdot \nabla(\zeta + f) = -(\bar{\mathbf{v}} - \mathbf{c}) \cdot \nabla \zeta' - \mathbf{v}' \cdot \nabla \zeta' - v'\beta. \quad (3.1)$$

In the f-plane experiment described in this subsection, the evolution of the vorticity pattern is determined solely by the term $-\mathbf{v}' \cdot \nabla \zeta'$ because $\mathbf{c} \approx \bar{\mathbf{v}}$ and $\beta = 0$. The effect due to the above term depends on the initial perturbation field, both its shape and intensity. If the initial shape of the disturbance is circular, this term would be zero, which would lead to no change in the initial vorticity field. This suggests that the initial perturbation shape may influence the shape of the evolving disturbance. In the cases with $\beta \neq 0$, the effect of the other two terms on the right side of (3.1), i.e., $-(\bar{\mathbf{v}} - \mathbf{c}) \cdot \nabla \zeta'$ and $-v'\beta$, can alter the shape of a disturbance even if $\mathbf{v}' \cdot \nabla \zeta' = 0$. Also note that if the basic flow has a vorticity gradient $\partial^2 \bar{u}/\partial y^2 \neq 0$, then the vorticity advection term would also contain the term $-\mathbf{v}' \cdot \nabla \bar{\zeta}$. This could also influence the disturbance shape but is not considered in this study.

The differences in the 48 h wind field among the dry, f-plane experiment (Fig. 8, lower right) and the two dry spherical cases (Fig. 9, right column) can be explained through the budget analysis of the relative vorticity ζ for these three experiments. Fig. 10 presents the horizontal distribution of the term $-(\mathbf{v} - \mathbf{c}) \cdot \nabla(f + \zeta)$ at 24 h. Fig. 10 (top) implies that, in case of the dry, f-plane experiment, the relative vorticity pattern

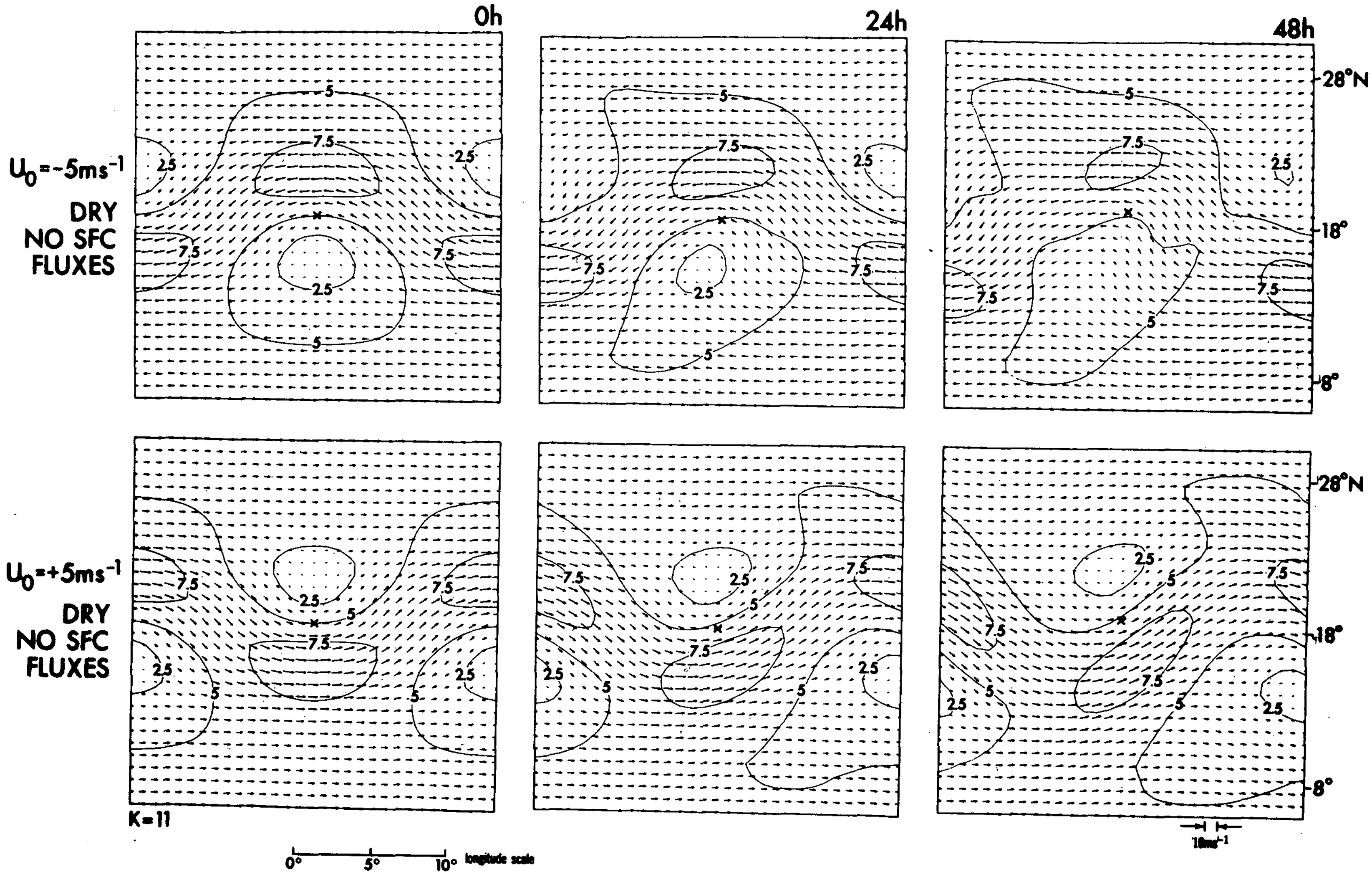

FIG. 9. Distribution of the low-level ($\sigma = 0.992$) wind vectors and isotachs (m s^{-1}) for two dry experiments with $\beta \neq 0$ and no surface fluxes. The experiment with $u_0 = -5$ m s^{-1} is shown at top and the experiment with $u_0 = +5$ m s^{-1} is shown at bottom for 0, 24, and 48 h respectively.

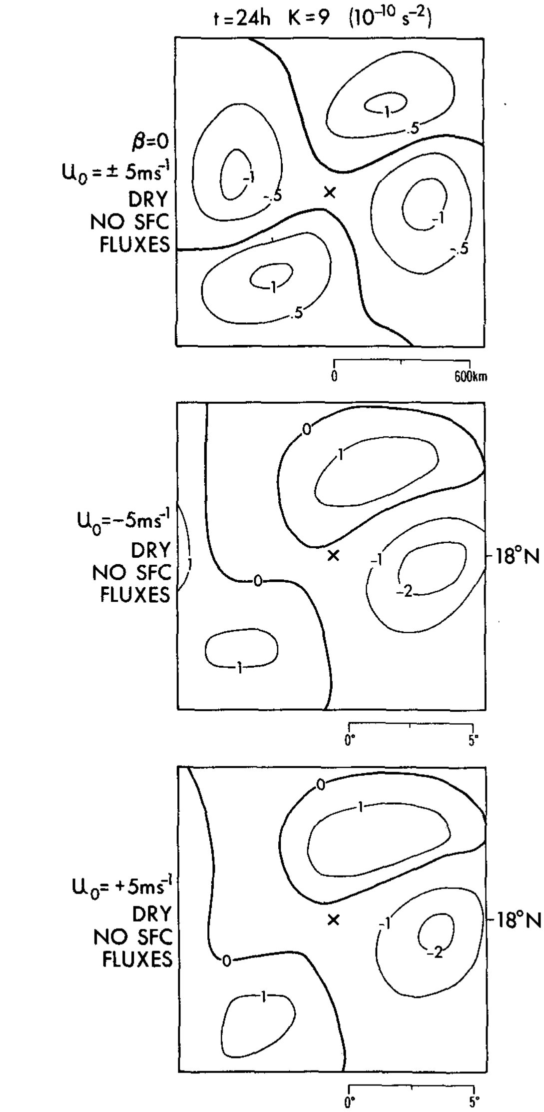

FIG. 10. The horizontal vorticity advection component of the vorticity tendency relative to the moving disturbance at 24 h for dry, no surface flux experiments with $u_0 = +5$ m s^{-1}, *f*-plane; $u_0 = -5$ m s^{-1}, $\beta \neq 0$; and $u_0 = +5$ m s^{-1}, $\beta \neq 0$ (top to bottom), respectively. In the *f*-plane experiments (top) identical patterns are obtained for the $u_0 = +5$ m s^{-1} and $u_0 = -5$ m s^{-1} cases. Units are in 10^{-10} s^{-2}.

rotates cyclonically, as stated previously, because of nonlinear advection. In the two spherical domain ($\beta \neq 0$) cases (i.e., $u_0 = -5$ m s^{-1}, Fig. 10 center; $u_0 = +5$ m s^{-1}, Fig. 10 bottom) the vorticity tendency patterns are nearly identical to each other and distorted compared to the *f*-plane case. It is found from inspection of the wind and vorticity distributions that the above dipole pattern obtained to the east of the vortex in the spherical model is caused by the vorticity advection terms $-v'\beta$ and $-(\bar{\mathbf{v}} - \mathbf{c}) \cdot \nabla \zeta'$. The vorticity tendency characterized by such a dipole pattern can induce the confluence of the westerlies and the diffluence of the easterlies. As a result, enhancement of the wind maxima occurs in the westerly wind case. However, changes, mainly in the curvature of the flow, take place in the easterly wind case. Thus the evolved wind fields in the two cases (Fig. 9) are dissimilar, as mentioned before.

In summary, one sees that in the dry, no surface flux experiments on an *f*-plane the wind pattern evolves through nonlinear advection of relative vorticity. In the spherical model, this advection tendency is distorted by the advection of planetary vorticity and by that of the disturbance vorticity by the mean relative flow, causing the dependency of comma shape development on the direction of basic flow. Thus a disturbance can be modified by vorticity advection through nonlinear advection and/or the β effect. In this respect, the initial pattern and intensity of the disturbance can influence the process of comma formation. In the nearly barotropic condition considered here, however, no significant mechanisms are available to concentrate the vorticity into a narrow band.

c. *Vorticity budgets for an intensifying and nonintensifying comma band*

Through some additional experiments with both condensation and radiation processes included, but with the surface fluxes of heat, moisture, and momentum excluded, it can be shown that the distinct comma band feature does not develop. These fluxes are essential for comma band formation. Low-level convergence due to surface friction increases the moisture convergence and intensifies the low-level vorticity. Evaporation helps maintain the high values of low-level equivalent potential temperature necessary for convective processes to become active in the disturbance region. On the other hand, we speculate that a vorticity band, if formed in the presence of surface fluxes but with no condensational heating, will be weak as the positive feedback process between surface convergence and condensational heating is absent. In the more realistic model experiments that include moisture, radiation and surface fluxes, the positive vorticity area is enhanced and concentrated. The vorticity budget analyses for these experiments are presented in the following.

The distributions of vorticity budget components at level 9 (~435 m) for the $u_0 + 5$ m s^{-1} and $u_0 - 5$ m s^{-1} cases in the experiments by TK (Section 1b and Section 2) are shown in Figs. 11 and 12, respectively, for 24 h. The twisting and vertical advection terms, negligibly small near the surface for both cases, are not shown. In contrast to the dry, no surface flux cases previously discussed, the net tendency in these experiments is no longer dominated by the relative advection term. This is especially true in the $u_0 = +5$ m s^{-1} case (Fig. 11). Furthermore, the magnitude of the major components of the vorticity tendency is as much as

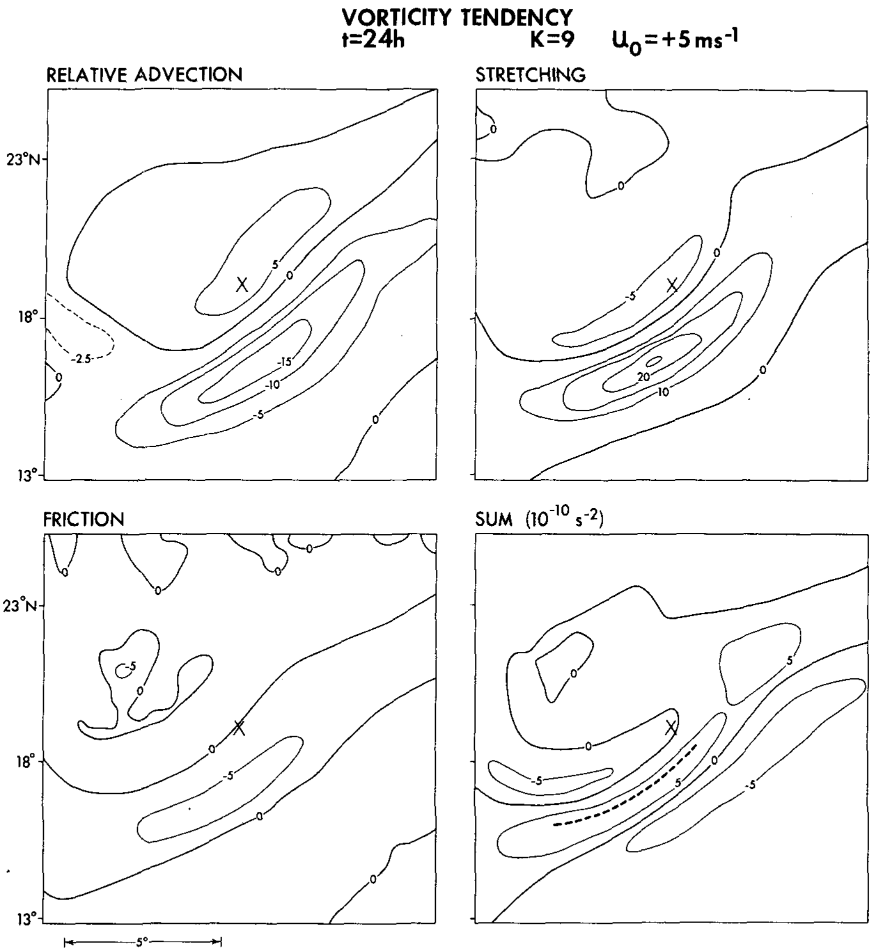

FIG. 11. Distribution of components and sum (10^{-10} s^{-2}) of the vorticity budget at level 9 (σ = 0.95), computed relative to the moving disturbance at 24 h for the experiment with $\beta \neq 0$ and u_0 = +5 m s^{-1} in which the comma pattern evolves. The vertical advection and twisting components are relatively small and not shown. Crosses indicate the surface position of the disturbance and the dashed line indicates the axis of the positive vorticity region.

an order of magnitude larger in this case than the net change in its dry, no surface flux analogue. Fig. 11 shows that the net effect of surface friction, vorticity stretching and relative advection results in a concentration of vorticity along the axis of the positive vorticity region, leading to the development of the distinct comma pattern. It is interesting to note that, although highly distorted, there still exists in the relative advection component, in both Figs. 11 and 12, a remnant of the four-cell pattern of the dry, f-plane, no surface flux case shown in Fig. 10 (top).

In the $u_0 = -5$ m s^{-1} case (Fig. 12), a net positive vorticity tendency does not occur along the full extent of the positive vorticity axis. The comma pattern, therefore, does not develop in the vorticity and wind fields for the $u_0 = -5$ m s^{-1} case as shown in Fig. 1 (top).

4. Remarks and conclusions

A detailed analysis of a numerically simulated tropical disturbance reveals at the mature stage a comma-shaped pattern in low-level vorticity, surface convergence, mid-level upward motion and precipitation. An analysis of the comma band reveals a low-level vorticity and surface pressure trough in the back half of the band and a wind shift, low-level convergence and mid-level upward motion centered along the band axis, if one defines the band as the region of precipitation. A rather strong southwesterly flow is observed along the leading edge of the band. Deep convection is an integral part of the band structure.

Earlier studies by TK have shown the formation of a comma vortex to be dependent on environmental flow direction. In case of easterlies little band devel-

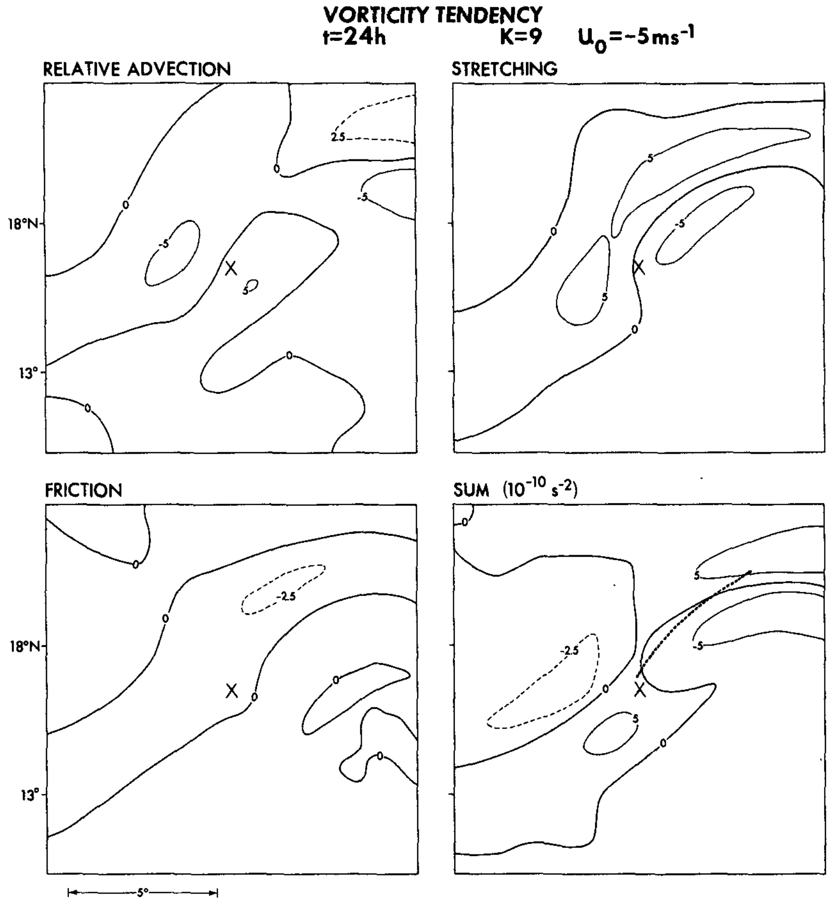

FIG. 12. As in Fig. 11 except for $u_0 = -5$ m s^{-1} in which the comma pattern was suppressed.

opment ensues. This study reveals that the β effect retards comma development in the case of easterlies and enhances it in the case of westerlies. The experiments on an f-plane indicate that without the β effect, comma vortices form with their bands on the high wind side of the disturbance regardless of flow direction.

The experiments with dry, no surface flux conditions produced band-like features in the wind field, especially with $\beta \neq 0$, $u_0 = +5$ m s^{-1}. However, these features were very weak. In contrast to the dry, no surface flux cases, the net vorticity tendency of the experiments which included moisture, radiation and surface fluxes is enhanced and concentrated near the band of the comma disturbance in case of westerlies. This results from the combined effects of relative advection of vorticity, vorticity stretching and surface friction. It is clear that surface fluxes of heat, moisture and momentum are vital ingredients for vorticity increase and concentration in the formative process of the distinct shape of the comma vortex.

Analysis of some simple dry experiments with no surface fluxes suggests that the initial shape and intensity of the disturbance can influence the evolution of the comma pattern. The initial shape of a perturbation in a uniform environmental flow may be altered by nonlinear vorticity advection as well as by the β effect. It can be speculated that the relative impact of the initial shape may be reduced for more realistic experiments which include moist processes and surface fluxes. An extensive investigation of this topic awaits further study.

At present, there is little conclusive observational evidence that shapes of tropical systems are determined by the mean basic flow. Systems with different shapes are observed and undoubtedly their structures are determined by more factors than just the mean environmental flow. Nonuniform momentum and moisture fields and the condition of the initial disturbance contribute to the shape of a disturbance. This numerical result does indicate, however, the potential impact of the flow direction in the comma shape formation.

A natural question arising from the present study is whether one can apply the mechanisms discussed in this study to the development of the extratropical comma vortices observed over oceans behind cold fronts. The mechanisms discussed in this study may have some legitimacy in the shaping of this feature even though the environmental condition of the extratropics is different from that of the tropics.

Acknowledgments. The authors would like to express appreciation to J. Smagorinsky and I. Orlanski for their support of the hurricane dynamics project. They wish to thank R. Shaginaw and F. Lipps of GFDL, T. Yamagata of the GFD Program of Princeton University, and J. Hoke of NMC for their comments on a preliminary version of this manuscript. P. Tunison, W. Ellis, M. Zadworney, K. Raphael, J. Conner and J. Kennedy provided valuable assistance in the preparation of this manuscript.

REFERENCES

Anderson, R. K., J. P. Ashman, F. Bittner, G. R. Farr, E. W. Ferguson, V. J. Oliver and A. H. Smith, 1974: Application of meteorological satellite data in analysis and forecasting. ESSA Tech. Rep. NESC 51 and November 1971 and March 1973 supplements. [NES, DIS, Suitland, MD 20233].

Anthes, R. A., and J. E. Hoke, 1975: The effects of horizontal divergence and the latitudinal variation of the Coriolis parameter on the drift of a model hurricane. *Mon. Wea. Rev.*, **103,** 757–763.

Brandli, H. W., 1976: Satellite meteorology. Air Weather Service Tech. Rep. AWS-TR-76-264. [Air Force Global Weather Center, Offutt AFB, NE 68113].

Dvorak, V. F., 1975: Tropical cyclone intensity analysis and forecasting from satellite imagery. *Mon. Wea. Rev.*, **103,** 420–430.

Hebert, P. J., 1980: Atlantic hurricane season of 1979. *Mon. Wea. Rev.*, **108,** 973–990.

Jones, R. W., 1977: Vortex motion in a tropical cyclone model. *J. Atmos. Sci.*, **34,** 1518–1527.

Kurihara, Y., and R. E. Tuleya, 1974: Structure of a tropical cyclone developed in a three-dimensional numerical simulation model. *J. Atmos. Sci.*, **31,** 893–919.

Lawrence, M. B., and J. M. Pelissier, 1981: Atlantic hurricane season of 1980. *Mon. Wea. Rev.*, **109,** 1567–1582.

——, and ——, 1982: Atlantic hurricane season of 1981. *Mon. Wea. Rev.*, **110,** 852–866.

Locatelli, J. D., P. V. Hobbs and J. A. Werth, 1982: Mesoscale structures of vortices in polar air streams. *Mon. Wea. Rev.*, **100,** 1417–1433.

Reed, R. J., 1979: Cyclogenesis in polar air streams. *Mon. Wea. Rev.*, **107,** 38–52.

Tuleya, R. E., and Y. Kurihara, 1981: A numerical study on the effects of environmental flow on tropical storm genesis. *Mon. Wea. Rev.*, **109,** 2487–2506.